Derivation of Force Field Parameters for TiO_2−H_2O Systems from ab Initio Calculations

A. V. Bandura[†] and J. D. Kubicki*[,‡]

St. Petersburg State University, St. Petersburg, Russia, and Department of Geosciences, The Pennsylvania State University, University Park, Pennsylvania 16802

Received: January 14, 2003; In Final Form: July 29, 2003

Periodic (CASTEP and DMol[3]) and cluster (Gaussian 98 and DMol[3]) ab initio calculations were carried out to develop force field parameters for the system Ti−O−H to model TiO_2−H_2O interfaces. A force field was derived from previously existing force fields for bulk TiO_2 polymorphs (Matsui, M.; Akaogi, M. *Mol. Simul.* **1991**, *6*, 239) and water (SPC/E; Berendsen, H. J. C.; Grigera, J. R.; Straatsma, T. P. *J. Phys. Chem.* **1987**, *91*, 6269) that describes Ti in a variety of coordination environments, Ti−O−H bonding, and H-bonding on TiO_2 surfaces. The force field was tested for its ability to reproduce ab initio structures of the hydrated (110) surface of α-TiO_2 (rutile).

Introduction

TiO_2 is an important material for its catalytic properties. Applications in photocatalytic processes for producing solar energy[1,2] and for treating contaminants in water[3,4] are two important reasons for understanding the surface of this material. Consequently, research has focused on TiO_2 polymorphs[5−7] and the surface chemistry of the predominant crystal faces.[8,9] The (110) face of rutile is of special interest because of its stability compared with other low index surfaces (100) and (001), and it was an object of several theoretical considerations using both Hartree−Fock (HF)[10] and density functional theory (DFT)[11−13] quantum mechanical ab initio approaches.

The motivation for this research effort is to help understand how the surface properties of TiO_2 affect the structure of water and counterions near the TiO_2/water interface. Developing force fields to describe Ti−O−H interactions is a first step in this direction. Force fields will allow larger scale simulations of the TiO_2/water interface that are not possible on an ab initio level. The complexity that is generated by the interactions among surfaces, water and dissolved ions requires that each component of the system be modeled accurately before attempting to model their interdependent behaviors. Hence, we begin by modeling the cleaved TiO_2 surface in a vacuum. These calculations are followed by hydration of the surface and testing whether associative or dissociative adsorption of H_2O is dominant.[8,9,14−16]

Methods

1. Testing Force Fields for TiO_2 Surfaces in a Vacuum. Several force fields are available for bulk TiO_2, but the under-bonded defect species that dominate the surface in vacuo may be not accurately modeled by these force fields. Hence, there is a need to test the applicability of force fields developed for bulk TiO_2 in modeling rutile surfaces. We have used two parametrizations in our trial set.[17,18] As shown by Oliver et al.[6] and by Yin et al.,[19] respectively, both force fields demonstrate the ability to reproduce the structure of TiO_2 polymorphs. Both tetrahedral and octahedral Ti coordination states exist in these polymorphs. Therefore, these force fields are reasonable starting points for the simulation of rutile surfaces. Both force fields describe the energy of crystal via central interatomic interactions and include electrostatic terms with short-range Buckingham potentials. Kim's force field includes an additional Morse term that represents covalent Ti−O bonds. Both force fields are compatible with the SPC/E water potentials[20] that we have chosen to describe H_2O in our model systems.

Calculations were performed with both parametrizations to determine which one would more accurately reproduce ab initio model rutile surfaces. To this end, a 3D-supercell consisting of 1×1 or 1×2 surface unit cells was used to model the (110) surface geometry (Figures 1 and 2). Our surface calculations employ the slab geometry, to which periodic boundary conditions are applied. This generates an infinite stack of quasi-2-dimensional slabs, each separated from its neighbors by a 10 Å vacuum gap. The thickness of the slabs is expressed in terms of a number of layers, where a layer is defined as a (110) plane that contains both Ti and O atoms. The smallest surface unit cell was chosen for pure surface calculations, having dimensions of $\sqrt{2}a$ (6.497 Å) and c (2.959 Å) in the ($\bar{1}10$) and (001) directions, respectively. The surface unit cell was doubled in the (001) direction for hydroxylated or hydrated surfaces. (Note: All 3-D calculations in this report were performed with cell parameters fixed to the experimental values.)

Two different slabs were considered for the cleaved (110) surface: one 3 Ti layers thick (vacuum gap 10 Å) and the second 5 Ti layers thick (vacuum gap 15 Å). These two slab thicknesses were chosen to test the effect of slab depth on calculated surface structures. The minimum energy structures of both slab models were determined using the generalized gradient approximation (GGA) of Perdew and Wang[21] (PW91) calculations within the CASTEP[22] module of Cerius[2] (Molecular Simulations Inc., San Diego, CA). Ultrasoft pseudopotentials[23] were used, allowing us to apply small plane wave cutoff energy −340 eV. The default CASTEP Monkhorst−Pack[24] scheme was used for choosing *k*-points. The positions of *all* atoms were allowed to relax for the 3 Ti layer slab, but the positions of atoms of the central layer were fixed at the bulk crystal geometry for the 5 Ti layer slab. In Figure 2 and Table 1, we compare the results for both slabs. The calculated structures do not depend greatly on the thickness of the slab. Hence, we conclude that the 3-layer

[†] St. Petersburg State University.
[‡] The Pennsylvania State University.

10.1021/jp034093t CCC: $25.00
Published on Web 09/16/2003

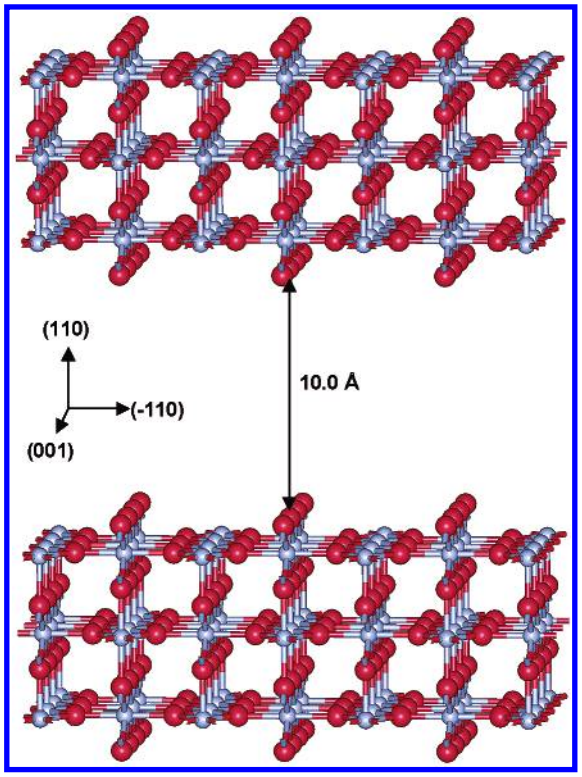

Figure 1. 3-Dimensional slab model of a TiO_2 (110) surface. Bulk crystal unit cell dimensions (Å): $a = 4.59$, $b = 4.59$, $c = 2.96$. Slab unit cell dimensions (Å): $a'(-110) = \sqrt{2}a = 6.50$, $b'(001) = c = 2.96$, $c'(110) = 19.03$.

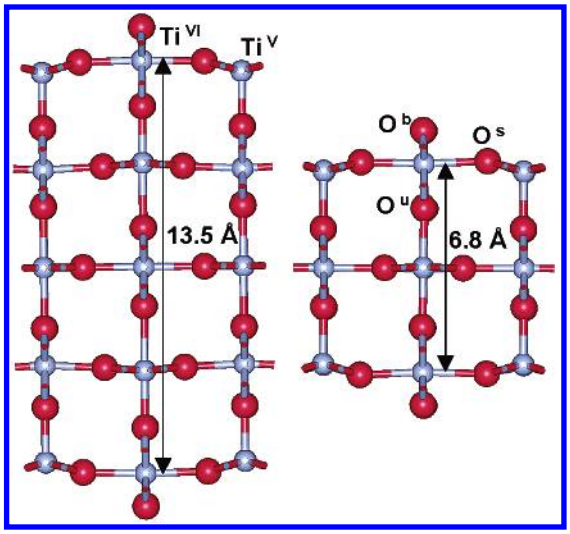

Figure 2. Comparison of the CASTEP-DFT-GGA-PW91-340 eV geometry optimization for 3-layer and 5-layer (with fixed positions of middle plane atoms) slabs of TiO_2.

slab is adequate for modeling the (110) surface to develop force field parameters.

The same starting structures were used for energy minimizations with each force field. Original parametrizations[17,18] developed for bulk crystal calculations were used in those calculations. A 9.6 Å cutoff distance was used for van der Waals interactions. In Figure 3, the results of a geometry optimization of the 3-layer slab using the force fields of Matsui and Akaogi[17] and Kim et al.[18] are shown and can be compared to the generated in the CASTEP[22] energy minimization (Figure 2). Both force fields are qualitatively correct in predicting surface relaxation of TiO_2. However, the first slightly underestimates and the second overestimates displacements of the outermost surface

TABLE 1: Calculated Bond Length (Å) on the Surface of the TiO_2 Slabs

Bond	DFT-GGA, 5-layer slab	DFT-GGA, 3-layer slab	FF Matsui,[17] 3-layer slab	FF Kim,[18] 3-layer slab
Ti(6f)−O(bridge)	1.82	1.83	1.85	1.79
Ti(6f)−O(term)	2.04	2.05	2.02	2.07
Ti(6f)−O(bulk)[a]	2.10	2.08	2.01	2.11
Ti(5f)−O(term)	1.94	1.93	1.92	1.91
Ti(5f)−O(bulk)	1.81	1.83	1.89	1.88

[a] Experimental Ti−O bond lengths in the bulk rutile crystal are 1.95 and 1.98 Å.

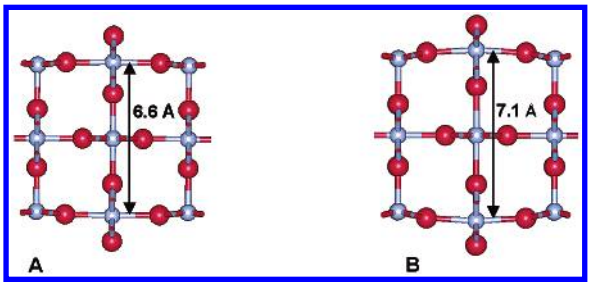

Figure 3. Comparison of surface relaxation for 3-layer slab obtained using different methods: (A) force field of Matsui;[17] (B) force field of Kim.[18] The numbers are the distances between 6-fold titanium atoms on the opposite surfaces of slab. The distance between the opposite-side 6-fold titaniums in unrelaxed 3-Ti-layer slab is 6.50 Å.

titanium atoms (Figure 3). Corresponding bond distances between the top surface atoms are given in Table 1. Either force field provides a reasonable starting point for modifying parameters to model surface Ti and O atoms.

2. Testing Force Fields for Hydration of TiO_2 Surfaces in a Vacuum. The Kim et al.[18] parametrization predicted atomic relaxations in the body of a hydroxylated (110) slab in disagreement with the GGA-PW91 structure (the development of the force field parameters for hydroxide groups will be described below). This can be seen in Figure 4a which shows the optimized structure of 3-layer slab with 4 hydroxyls using the Kim et al. force field. There was less discrepancy between the Matsui and Akaogi[17] parametrization and the GGA-PW91 results (Figure 4b). Another test of the force fields was based on calculations of small titanium hydroxide complexes (Figure 5). Using both the above-mentioned force fields, the parametrization of Matsui and Akaogi[17] again was favorable. Also, the Ti and O charges obtained by CHelpG analysis[26] of MP2/6-311+G(d,p) calculations on the different titanium hydroxide complexes [$Ti(OH)_4$, $Ti(OH)_4(H_2O)$, and $Ti_2(OH)_8(H_2O)_2$] were closer to Matsui and Akaogi's[17] charges than to those of Kim[18] (Figures 5 and 6). Consequently, we decided to use the parametrization[17] as a starting point for our TiO_2 surface force field. Original parameters derived for bulk TiO_2[17] are given in Table 2.

3. Parameters for the Ti−OH Group. One important problem is to describe the interactions of bonded OH groups with neighboring atoms on a TiO_2 surface. In this case, a simple two-body central-force potential is not valid. Two relatively simple possibilities exist for reproducing the directionality of OH bonds: (1) introducing oxygen polarizability via the shell model of Dick and Overhauser[27] or (2) introducing bond stretching and angle bending terms for Ti−O−H. The shell model is now widely used for atomic modeling of hydroxide ions in inorganic solids[28,29] and for molecular dynamics (MD) simulations of chemisorption of water on oxide surfaces.[30,31] However, the shell model may not be wholly consistent with the SPC/E H_2O force field (Table 3). Consequently, we decided

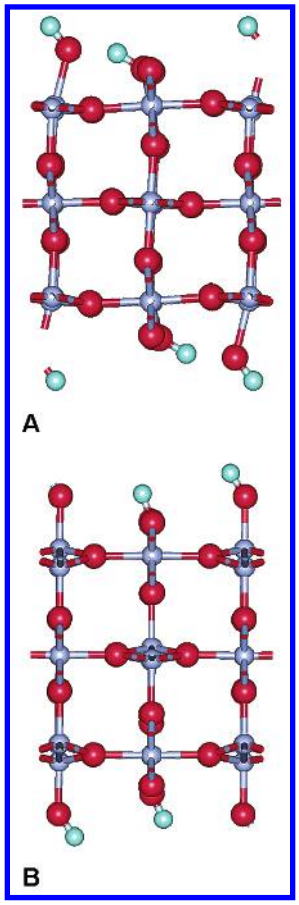

Figure 4. Structural comparison of 3-layer slabs with four hydroxyls using different force field parameters: (A) Matsui and Akaogi;[17] (B) Kim et al.[18]

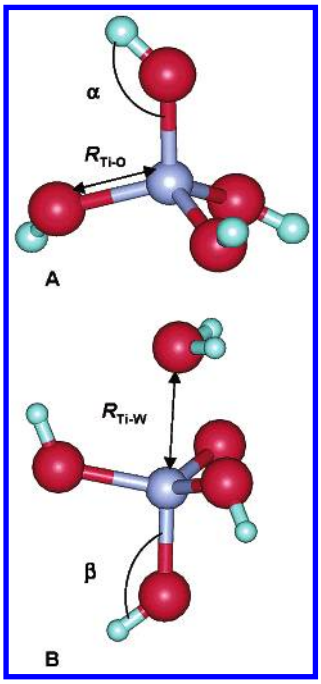

Figure 5. Optimized structures for $Ti(OH)_4$ (A) and $Ti(OH)_4(H_2O)$ (B). Gaussian98-MP2/6-311+G(d,p): $R_{Ti-O} = 1.81$ Å, $\alpha = 133°$, $R_{Ti-W} = 2.38$ Å, $\beta = 128°$. DMol^3-DFT-GGA-BLYP: $R_{Ti-O} = 1.85$ Å, $\alpha = 125°$, $R_{Ti-W} = 2.65$ Å, $\beta = 129°$. Force field calculations using the force field derived in this work: $R_{Ti-O} = 1.81$ Å, $\alpha = 132°$, $R_{Ti-W} = 2.56$ Å, $\beta = 128°$.

to use bond-stretching and angle-bending terms to model the Ti−O−H.

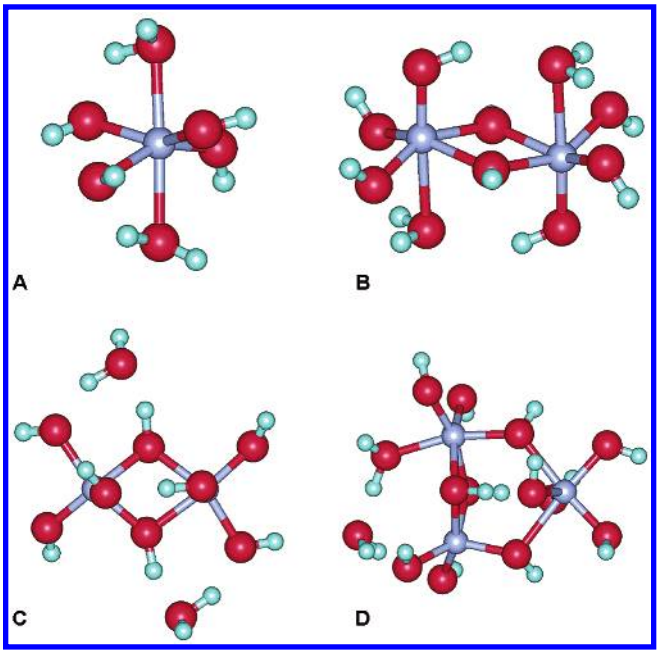

Figure 6. Structures used for obtaining the CHelpG charges: (A) $Ti(OH)_4(H_2O)_2$, structure with 6-fold coordinated Ti; (B) $Ti_2(OH)_8(H_2O)_2$, structure with 6-fold coordinated titanium; (C) $Ti_2(OH)_8(H_2O)_2$, structure with 5-fold coordinated titanium; (D) $Ti_3(OH)_{12}(H_2O)_2$, structure with two 6-fold coordinated titanium and single 5-fold coordinated titanium atoms.

TABLE 2: Parameters of Buckingham Potential[17,a] ($E_{ij} = A_{ij} \times \exp(-r_{ij}/\rho_{ij}) - C_{ij}/r_{ij}^6$)

$i-j$	A_{ij}, kcal mol^{-1}	ρ_{ij}, Å	C_{ij}, kcal mol^{-1} Å^6
Ti−O	391049.1	0.194	290.3317
Ti−O[b]	315480.8	0.194	290.3317
Ti−Ti	717647.4	0.154	121.0676
O−O	271716.3	0.234	696.8883
Ti−O(H_2)[c]	28593.02	0.265	148.000[d]

[a] Bulk atomic charges: $q(Ti) = 2.196$, $q(O) = -1.098$. [b] Modified potential[17] for terminal hydroxyl obtained in small hydroxide complexes. [c] Interaction between the water oxygen and Ti atom approximated by Buckingham function. [d] Value of Ti−O dispersion coefficient has been estimated from polarizabilities of Ti^{4+} ion and water molecule (see text).

TABLE 3: Parameters of Water−Water Potential[20,a] ($E_{ij} = q_iq_j/r_{ij} + \epsilon_{ij}[(\sigma_{ij}/r_{ij})^{12} - 2(\sigma_{ij}/r_{ij})^6]$)

$i-j$	ϵ_{ij}, kcal mol^{-1}	σ_{ij}, Å
O^w-O^w	0.15539	3.5532
O^w-H^w	0.000	
H^w-H^w	0.000	

[a] Atomic charges: $q(O^w) = -0.8476$, $q(H^w) = 0.4238$.

Variations of the Morse potential are available[28,29,32,33] for O−H bond stretching vibrations. The Morse potential of Fleming et al.[29] produces reasonably accurate bond lengths and the vibrational frequencies of O−H in $Ti(OH)_4$ and in other titanium hydroxide complexes (Table 4). We applied the potential of Fleming et al.[29] to (Ti)O−H bonds without any modifications (Table 5). Note that there are no intramolecular Coulomb interactions between bonded oxygen and hydrogen within hydroxyl groups as well as between all atoms of H_2O molecules.

For the Ti−O−H angle-bending term, the harmonic approximation was used. Coulomb interactions between the titanium and hydrogen atoms bonded to common oxygen are strong. These next-nearest neighbor Coulomb interactions are usually omitted in most molecular mechanics force fields but

TABLE 4: Vibrational Frequencies for Titanium Hydroxide Complexes (cm^{-1})

$Ti(OH)_4$				$Ti(OH)_4(H_2O)$			$Ti_2(OH)_8(H_2O)_2$		
no.	DFT/GGA-BLYP	MP2/6-311+G**	force field	no.	DFT/GGA-BLYP	force field	no.	DFT/GGA-BLYP	force field
16	501.2	426.2	585.9	21	522.1	459.0	41	528.4	539.5
17	508.0	426.2	647.4	22	525.8	574.8	42	537.1	558.2
18	528.4	428.2	669.8	23	572.3	620.6	43	553.2	567.9
19	535.7	437.8	669.8	24	600.3	660.0	44	559.1	583.4
20	645.7	709.5	714.3	25	607.8	672.6	45	582.6	599.7
21	714.2	764.3	715.5	26	618.2	700.4	46	592.9	603.9
22	734.7	782.4	733.4	27	693.9	716.7	47	595.7	612.3
23	738.5	782.4	733.4	28	706.6	732.7	48	604.1	630.9
24	3716.0	3937.8	3734.2	29	721.9	745.5	49	630.4	641.1
25	3718.7	3938.2	3734.2	30	1615.9	1629.0	50	636.9	652.2
26	3725.3	3938.3	3734.3	31	3611.6	3589.7	51	644.7	676.6
27	3730.2	3946.5	3742.2	32	3710.2	3656.0	52	651.1	683.4
				33	3711.1	3708.4	53	670.6	728.7
				34	3711.8	3724.5	54	684.6	739.1
				35	3712.0	3729.2	55	698.0	816.4
				36	3718.0	3737.2	56	714.9	827.0
							57	793.7	839.1
							58	798.6	849.3
							59	1632.2	1632.2
							60	1632.2	1632.4
							61	3601.5	3549.0
							62	3601.8	3551.2
							63	3642.0	3612.3
							64	3643.5	3613.9
							65	3701.2	3622.3
							66	3701.3	3626.0

TABLE 5: Parameters of the O−H Morse Potential ($E_{ij} = A_{ij}\{1 - \exp[-\alpha_{ij}(r_{ij} - r_{ij}^0)]\}^2 - A_{ij}$)

$i-j$	A_{ij}, kcal mol^{-1}	α_{ij}, $Å^{-1}$	r_{ij}^0, Å	ref
(H)O−H	101.905	2.3470	1.00	this work[a]
(Ti)O−H	125.094	2.2682	0.95	29

[a] A_{ij} and r_{ij}^0 from ref 33.

TABLE 6: Parameters of the H−O−H and Ti−O−H Angle Bending ($E_{ijk} = (1/2)k_2(\theta - \theta_0)^2$)

i	j	k	θ_0, deg	k_2, kcal mol^{-1} rad^{-2}
H	O	H	109.47	103.045
Ti	O	H	90.85	14.136

must be included in our force field because it is based on an ionic model of the solid oxide. (Excluding of Coulomb interactions was possible only if the additional angle-bending and torsion parameters were introduced for all other possible angles.) To obtain the corresponding force constants, we performed quantum mechanical calculations on $Ti(OH)_4$ and on other small titanium hydroxide complexes (Figure 5), using different levels of theory: LDA-PWC, GGA-BLYP, and MP2/6-311+G(d,p) (the first two within DMol^3 [25] and the third within Gaussian 98[34]). The first approximation runs efficiently and results in structures that are close to the MP2/6-311+G(d,p) results. The GGA-BLYP (the generalized gradient approximation, the Becke exchange correlation functional,[35] and Lee−Yang−Parr correlation functional[36]) calculations were performed using DMol^3 and the DNP all-electron basis set was used instead of the pseudopotential method. The DNP basis set was used in the LDA-PWC calculations, but the pseudopotential method was employed in this case. GGA-BLYP theory[35,36] was also used to estimate vibrational frequencies of the titanium hydroxide complexes.

The force constants k_2 and angle parameter θ_0 given in Table 6 were adjusted to reproduce the structure and vibrational frequencies (on average) for $Ti(OH)_4$ obtained by GGA-BLYP calculations (Table 4). Force field parameters were adjusted to fit the DFT results with the Generalized Utility Lattice Program (GULP;[37]). The Buckingham parameter A_{TiO} has been also adjusted to improve the Ti−O bond length in this complex (Table 2). The vibrational frequencies have been included explicitly as well as the equilibrium atomic positions in empirical fitting procedure using GULP program with the "RELAX" keyword. We used the MP2/6-311+G(d,p) CHelpG[26] charges for all atoms in those calculations. Values of k_2, θ_0, and A_{TiO} depend on their initial guess, so two other species, $Ti(OH)_4(H_2O)$ and $Ti_2(OH)_8(H_2O)_2$ (see section 5), have been used to choose the best set. The final structures obtained using the GULP cluster optimization are very close to those shown in Figure 5 and corresponding frequencies are given in Table 4.

4. Parameters for Ti−O−H_2O Interactions. The next aspect of our calculations involved testing various possible hydration models and predicting the stability of each hypothesized model after hydration and structural relaxation. The SPC/E model of water[20] (Table 3) will be used for H_2O-H_2O interactions, but parameters for H_2O-TiO_2 surface interactions had to be derived. For this purpose, H_2O−Ti interaction parameters were extracted by fitting to structures obtained via DMol^3 [25] calculations using GGA-BLYP, on molecular cluster $Ti(OH)_4(H_2O)$. We used the MP2/6-311+G(d,p) CHelpG[26] charges for titanium species in those calculations, whereas, the charges on the water molecules were set equal to those of SPC/E force field. We have found that the potential form derived by Curtiss[38] and used by Guardia and Padro[39] for MD calculations of $Fe^{3+}-H_2O$ can be used as a starting point for the Ti^{4+}−O pair interaction. The Curtiss[38] potential was re-fitted to a Buckingham form and used as an initial guess for adjusting the structure and vibrational frequencies to fit values for $Ti(OH)_4(H_2O)$ obtained with GGA-BLYP calculations (Table 4). The dispersion coefficient C_{TiO} was estimated theoretically using approach of Fowler et al.[40] from polarizabilities of Ti^{4+} ion and a H_2O molecule. We have used the value of 0.22 $Å^3$ for polarizability of Ti^{4+} that was obtained by Calderwood.[41] Static dipole polarizability of water molecule (1.47 $Å^3$) and water−water isotropic dispersion coefficient (625.2 kcal mol^{-1} $Å^6$) that are needed for estimation were taken from the work of Cohen

TABLE 7: Vibrational Frequencies for H_2O (cm^{-1})

band	DFT/GGA-BLYP	MP2/6-311+G(d,p)	exp, gas phase	force field
H−O−H	1612.6	1628.6	1595	1611.8
O−H	3677.7	3883.6	3657	3701.9
	3791.5	4002.4	3756	3774.5

and Saykally.[42] It should be noted that the H_2O-H_2O isotropic dispersion coefficient from[42] is close to the C_{OO} coefficient of the SPC/E water model (625.4 kcal mol^{-1} $Å^6$).

The resulting Buckingham parameters for $Ti^{4+}-O(H_2)$ interactions are given in the Table 2. The $O(H_2)-O(Ti)$ van der Waals interactions were set equal to the O−O interactions for H_2O-OH_2 in the SPC/E force field.

The SPC/E force field for H_2O[20] is rigid, and this fact introduces some inconvenience in the force field calculations when the structure and parameter optimizations are needed. For example, the GULP program[37] does not permit rigid molecules to be used in geometry optimization. Hence, we introduced additional intramolecular terms in the water potential for the purpose of deriving the force field parameters. Starting from the Toukan and Rahman[33] intramolecular potential, we replaced the original harmonic term[33] for displacement of atomic sites from their equilibrium distances by a term for the deviation of bond angle from its equilibrium value in the SPC/E force field. The harmonic and Morse potential parameters have been adjusted using the GULP program[37] to reproduce the results of GGA-BLYP[35,36] calculations of vibrational frequencies in the gas-phase water molecule. This approximation has been shown by Bergstrom and Lunell[43] to be successful in predicting the structure and vibrational frequencies of titanium oxide molecules, so we used it for our frequency calculations of the titanium hydroxide complexes. For compatibility reasons, we have applied the GGA-BLYP theory[35,36] to calculate water vibrations as well.

The vibrational frequencies of water obtained by different methods are given in Table 7. The derived parameters for water are in Tables 5 and 6. The absolute values of intramolecular terms do not influence significantly the geometrical and energy parameters of the systems in which the H_2O molecules are involved. Thus, the energy of a H-bond in the H_2O-H_2O dimer calculated using parameters from Tables 3, 5, and 6 is 7.5 kcal/mol, whereas the rigid SPC/E force field gives 7.2 kcal/mol. The results of the calculations of other hydrated species will be discussed in the next sections. The formation energy calculated with our force field parameters (without a zero-point correction) for $Ti(OH)_4(H_2O)$ is equal to −9.2 kcal/mol, which compares reasonably well with the GGA-BLYP result of −7.2 kcal/mol.

Values obtained from these cluster calculations were then tested for use on periodic surfaces by our CASTEP calculations of a H_2O molecule adsorbed on the relaxed TiO_2 surfaces. Results of DFT studies of water adsorption on TiO_2 obtained by Stefanovich et al.,[16] Vogtenhuber et al.,[44] Casarin et al.,[45] and Goniakowski et al.[46] were also taken into account, as well as the first-principles molecular dynamics calculations of Lindan et al.[14,15]

5. Derivation of Charges for Surface Atoms. Information on the surface charges may be obtained using standard population analysis based on results of periodic slab calculations. However, the Mulliken charges cannot be used directly for several reasons: (1) they depend to a large extent on the basis set (especially on hydrogens) and other details of method used; (2) they do not match the original force field charges that have been adopted; (3) they are sensitive to geometry of system. Also, the Mulliken charges in plane-wave CASTEP calculations are produced by indirect projection technique. Another problem arises from the fact that charges will be required both for the neutral and charged surface systems.

Our preferred choice was to use the electrostatic potential of the 3-D surface system as additional property for charge-fitting procedures. Unfortunately, we could not obtain reliable electrostatic potentials for 3-D TiO_2 systems using CASTEP or DMol[3]. To overcome this difficulty, we decided to use charges obtained from calculations on clusters that approximate rutile surface species. First, we have used clusters in which atoms preserve their positions at bulk crystal geometry. However, there are at least two problems that prevent employing these clusters for charge derivations. The first is originated in dangling bonds or excess charge that is usually attributed to small clusters. We have investigated different means to saturate the dangling bonds and neutralize the excess charge using hydrogen, lithium, or magnesium atoms. Nevertheless, we could not obtain sufficiently simple charge distributions that could be used in surface slabs. The second problem arises when we use significantly larger clusters made up from multiple rutile unit cells. The electrostatic potential outside the cluster becomes insensitive to the charges of atoms in the center of the cluster (i.e., only atoms on the surface of the cluster contribute to the CHelpG fitted electrostatic potential). Therefore, derived charges for larger clusters cannot be obtained without additional constraints. Given this situation, other systems were used for the charge-fitting procedure as described below.

Quantum mechanical calculations were carried out on four systems (Figure 6): $Ti(OH)_4(H_2O)_2$, $Ti_2(OH)_8(H_2O)_2$ (two different conformations), and $Ti_3(OH)_{12}(H_2O)_2$. These systems include 5- and 6-fold coordinated Ti, hydroxyl groups, and H_2O molecules. The structures calculated above correspond to definite local energy minima as revealed by frequency analysis of each structure. They have been chosen to represent different environments of surface titanium atoms. The geometry optimizations were performed using LDA-PWC functionals. Then, CHelpG charges were evaluated using the MP2/6-311+G(d,p) basis set in Gaussian 98. Thus, the derived charges represent the electrostatic potential around the clusters, but the cluster approximation needs to be tested in this case (i.e., a comparison of charges derived from clusters and periodic models needs to be made).

First, to obtain values of charges on the titanium atoms, hydroxyl oxygens, and hydrogens, the average charge values on each type of center were calculated. The original charges and their mean values are given in Table 8. Also, the mean value of charge on H atoms of water molecules involved in clusters is given in the last column of Table 8. Then, a simple procedure was used to obtain the final charges. The mean values of the oxygen and hydrogen charges in Ti species were scaled such that the mean charge on water H atoms became equal to value in the SPC/E water model. In other words, we multiply the mean charges by the ratio $q(H^w)/q(H^{h2o})$, where $q(H^w) = 0.4238\ e$ (the SPC/E value) and $q(H^{h2o}) = 0.4529\ e$ (the mean charge for water hydrogen in hydroxide complexes). This ensures the equality of scales for oxygen and hydrogen charges both for water and surface groups. The resulting charges are given in the last row of Table 8. To obtain other charges on the surface atoms, we regarded the charge balance for two extreme cases of neutral rutile surface: (1) a relaxed, in vacuo surface and (2) a fully hydroxylated surface. Also, we assumed that the charge on 3-fold coordinated surface oxygen atoms equals the "bulk" value and that all surface Ti atoms have equal

TABLE 8: CHelpG Charges on the Atoms of Titanium Clusters

N	Ti	O^{bh}	O^{oh}	H^{bh}	H^{oh}	H^{h2o}
1	2.156	−1.069	−1.026	0.435	0.481	0.395
2	2.283	−1.053	−1.052	0.478	0.481	0.369
3	2.072	−1.026	−0.969	0.653	0.447	0.459
4	2.076	−1.162	−1.026	0.421	0.447	0.384
5	2.076	−1.079	−1.052	0.513	0.466	0.464
6	2.018	−0.892	−0.969	0.453	0.466	0.455
7	2.018	−0.978	−1.002	0.468	0.470	0.464
8	2.282	−0.978	−1.041	0.468	0.455	0.455
9			−1.042		0.490	0.475
10			−1.000		0.455	0.392
11			−1.089		0.449	0.440
12			−1.067		0.575	0.451
13			−1.048		0.426	0.477
14			−0.990		0.440	0.598
15			−0.979		0.472	0.484
16			−0.967		0.484	0.485
17			−0.949		0.424	
18			−0.957		0.453	
19			−1.041		0.429	
20			−0.930		0.442	
21			−1.007		0.417	
22			−1.004		0.426	
23			−0.916		0.477	
24			−0.976		0.439	
mean	2.123	−1.030	−1.004	0.486	0.459	0.4529
scaled	1.986	−0.964	−0.939	0.455	0.430	0.4238

charges. These assumptions are in qualitative accordance with the results of available HF periodic calculations of Reinhardt and Hess[10] that showed only a small reduction of Mulliken charges on 5- and 6-fold Ti atoms and slightly larger deviations on bridging oxygen atoms. Our own computations[47] agree with this picture. Thus, the procedure below was adopted for estimating the charges for all surface atoms.

(i) For bridging oxygens (O^{bh}), terminal hydroxyl oxygen (O^{oh}), bridging hydrogen (H^{bh}), and terminal hydroxyl hydrogen (H^{oh}), the scaled average values obtained in the cluster calculations were used (Table 8).

(ii) The original force field value[17] of oxygen charge −1.098 *e* was used for the charges on the 3-fold coordinated oxygen atoms in the Ti surface layer (O^{s}) and under the Ti surface layer (O^{u}).

(iii) To obtain the charges on 5-fold coordinated titanium (Ti^{V}), on 6-fold coordinated titanium bonded to hydroxyl (Ti^{VIoh}), and on 6-fold coordinated titanium (Ti^{VI}) we considered the following neutrality condition:

$$[q(Ti^{VIoh}) + 2q(O^{s}) + q(O^{oh}) + q(H^{oh})] + [q(Ti^{VI}) + q(O^{u}) + q(O^{bh}) + q(H^{bh})] = 0 \quad (1)$$

with the assumption that $q(Ti^{VIoh}) = q(Ti^{VI}) = q(Ti^{surf})$. This yields $q(Ti^{surf}) = 2.156$ *e*.

(iv) Using the same assumption, the neutrality condition for in vacuo surface

$$[q(Ti^{V}) + 2q(O^{s})] + [q(Ti^{VI}) + q(O^{u}) + q(O^{b})] = 0 \quad (2)$$

gave the value for $q(O^{b}) = -1.018$ e.

Applying the procedure above, charges were obtained that reproduced the structure of the relaxed hydroxylated slabs more accurately than the original charges[17] and that take into account the electrostatic potential near the Ti−hydroxide complexes. The resulting values are given in Table 9. Derived charges correctly describe the H-bond structure of the hydroxylated surface, but they are unable to compensate entirely for the small surface relaxation attributed to the original parametrization[17] and to reproduce the elevated position of hydroxylated Ti. Additional computations may be needed to improve upon these results.

TABLE 9: Derived Charges on the Surface Atoms

atom	charge	atom	charge	atom	charge
Ti^{a}	2.196	O^{a}	−1.098		
Ti^{V}	2.156	O^{b}	−1.018		
Ti^{VI}	2.156	O^{s}	−1.098		
Ti^{VIoh}	2.156	O^{u}	−1.098		
		O^{bh}	−0.964	H^{bh}	0.455
		O^{oh}	−0.939	H^{oh}	0.430

[a] Original bulk value.

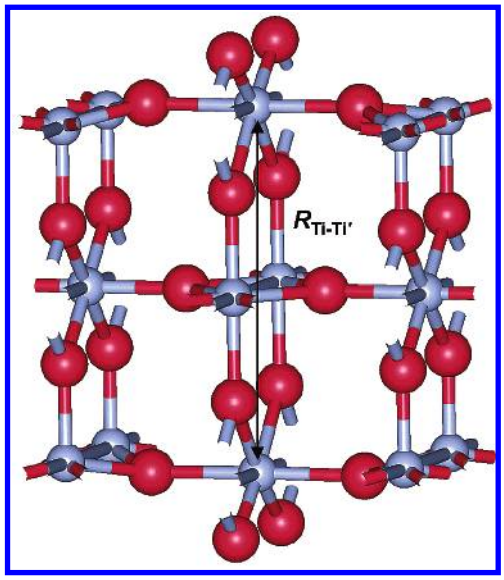

Figure 7. Optimized structure of 3-layer slab (model I). The distance between the opposite-side 6-fold titaniums: for CASTEP-DFT-GGA-PW91-340 eV calculations $R_{Ti-Ti} = 6.79$ Å, and for force field calculations with additional parameters for surface atoms $R_{Ti-Ti} = 6.73$ Å.

6. Modification of Parameters for Surface Atoms. CASTEP calculations were performed on several TiO_2 slabs that represent the relaxed in vacuo and hydroxylated rutile surfaces (Figures 1, 2, and 7−9). Inversion symmetry (space group *P*2) was imposed on all investigated systems to eliminate the total dipole moment. Generation of dipole moments within a slab can dramatically alter the results of 3-D periodic calculations,[48] so this methodology was adopted to minimize this problem. In most cases, we performed calculations for 3-layer slabs with a thickness ≈9 Å. Two different methods of structural relaxation (models I and II) were used for 3-D slabs (Figures 8 and 9). The positions of all atoms were allowed to relax for model I, but the positions of atoms of the central layer were fixed at the bulk crystal geometry for model II. As have been shown by Bates et al.[13] and by Zhang et al.,[49] four layer slabs may well be adequate for many purpose, but satisfactory convergence is only achieved for slabs of six or seven layers. Due to the computational restrictions we could not use such multilayer slabs in our set of calculations. Thus, one should keep in mind that results obtained for 3-layer systems may not represent all details of relaxations in real crystal surface as well as the exact adsorption energies. Especially, this may concern the displacements of atoms of the central layer that is equally disposed from both faces of the slab on the short distance. Because of this, model II may be more realistic for thin slabs than model II. Similar structures have been studied in other theoretical investigations,[14−16,44−46] and these surfaces have been studied experimentally.[8,9,50] Consequently, we have a significant amount

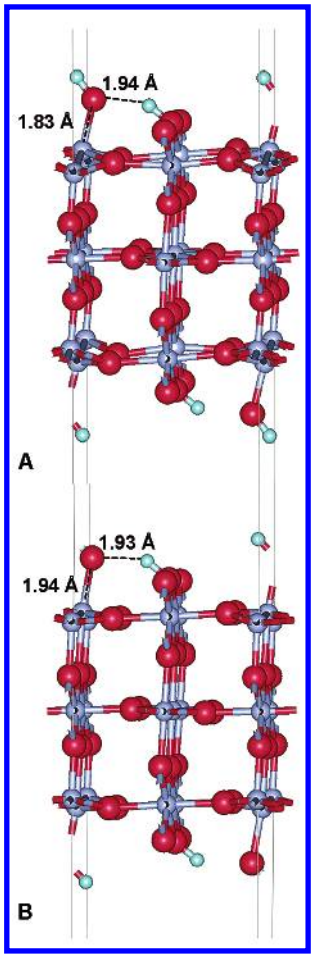

Figure 8. Optimized structure of a 3-layer slab with the bridging and terminal hydroxyls (model I, half-monolayer coverage) using (A) CASTEP-DFT-GGA-PW91-340 eV and (B) force field calculations.

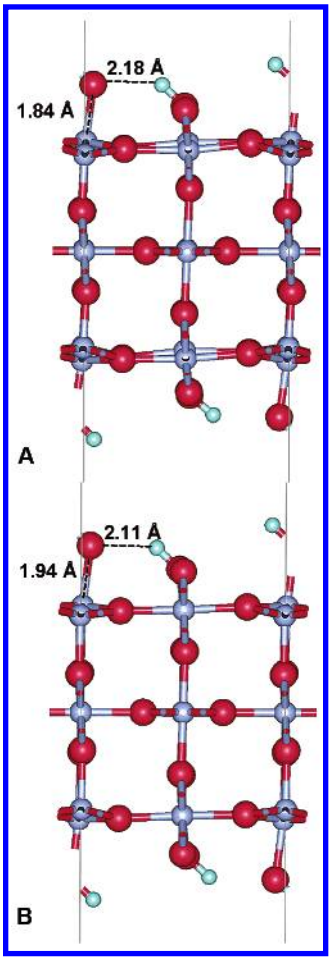

Figure 9. Optimized structure of hydroxylated 3-layer slab with fixed positions of the central plane atoms (model II, half-monolayer coverage) using (A) CASTEP-DFT-GGA-PW91-340 eV and (B) force field calculations.

of structural data for rutile surfaces with which to compare our results. However, future studies with thicker slabs may be necessary to alleviate this problem.

The next step in our force field development was to derive atomic charges for surface atoms that would predict accurately the electrostatic potential at the TiO_2−water interface (a key parameter in the description of counterion structure of the electrostatic double layer). To improve agreement between our force field and DFT structures of relaxed TiO_2 surfaces, an adjustment of the Buckingham parameters for Ti−O and O−O interactions on surface atoms was performed. Preliminary analysis showed that atomic relaxation is most sensitive to the parameters of Ti^{V}−O and O^{s}−O interactions. Hence, revised values of Buckingham A_{ij} for these atomic pairs were derived that differ slightly from the original[17] values and do not change the Buckingham parameter ρ_{ij} and coefficient C_{ij} for the long-range dispersion term. For simplicity, the A_{TiO} parameter determined previously for Ti−O bonds in the small Ti−hydroxide complexes has been used for the Ti^{VIoh}−O^{oh} term. The DFT structure of the in vacuo TiO_2 slab (Figures 2 and 7) has been chosen on the first stage of the fitting procedure using GULP. Then, the obtained parameters were used as initial guesses for fitting the quantum mechanical results on the hydroxylated model (I) (Figure 8a) and the final parameter set was produced. Previously derived charges have been used in all fitting procedures. We have found that it is sufficient to change only three Buckingham A_{ij} for O^{s}-involved interactions to improve significantly the agreement between the DFT and force field optimized structures. Derived parameters are given in Table 10. The optimized structures of the pure TiO_2 (110) surface obtained using DFT and our force field are similar (Figure 7). Corresponding results for hydroxylated models I and II are shown in Figures 8 and 9. The significant improvement can be seen from these pictures in comparison with the results obtained using the original[17] parameters (Figures 3 and 4). However, it was difficult to reproduce the correct length of Ti^{VIoh}−O^{oh} bond. The $A_{Ti^{V}O}$ parameter determined previously for Ti−O bonds in the small Ti−hydroxide complexes improves agreement but not to the desired extent. Nevertheless, our force field correctly predicts the orientation of hydroxyl groups on TiO_2 (110) surface both for half-monolayer (Figures 8 and 9) and full-monolayer (Figure 10) adsorption.

TABLE 10: Additional Parameters of Buckingham Potential for Surface Atoms of Titanium Oxide[a] ($E_{ij} = A_{ij}\exp(-r_{ij}/\rho_{ij}) - C_{ij}/r_{ij}^6$)

$i-j$	A_{ij}, kcal mol^{-1}	ρ_{ij}, Å	C_{ij}, kcal mol^{-1} Å^6
Ti^{VIoh}−O^{oh}	315480.8	0.194[b]	290.3317[b]
Ti^{c}−O^{s}	449223.3	0.194[b]	290.3317[b]
O^{d}−O^{s}	570799.0	0.234[b]	696.8883[b]
O^{s}−O^{s}	150150.9	0.234[b]	696.8883[b]

[a] Original[17] parameters have been used for other Ti−O, for O−O, and for all Ti−Ti interactions. [b] Original[17] values. [c] Titanium atom allowed to have any type. [d] Oxygen atom allowed to have any type.

7. TiO_2−H_2O Interactions. Adopting the first-order approximation for a TiO_2−H_2O potential mentioned in the section 2, we simulated the adsorption of one and two pairs of H_2O molecules (i.e., one or two on each side of the slab) with the 3-

TABLE 11: Calculated (without Zero Point Correction) and Experimental Adsorption Energies for $H_2O/TiO_2(110)$ (kcal/mol)

method		molecular adsorption	dissociative adsorption	ref
DFT-GGA-PW91, 340 eV	340 eV, model II, 3 Ti layer slab	21.5[a]	26.5[a]	this work
	340 eV, model II, 3 Ti layer slab	24.9[b]	23.0[b]	
	340 eV, model II, 5 Ti layer slab	21.7[b]	18.4[b]	
force field calculations	model II, 3 Ti layer slab	28.9[a]		this work
	model II, 3 Ti layer slab	26.3[b]		
	model II, 5 Ti layer slab	25.2[b]		
DFT-GGA-BP88, 1000 eV		18.9[b]	24.9[b]	46
DFT-GGA-BP88, 750 eV 3 Ti layer slab			31.13[a]	14
		31.3[c]	37.3[c]	
B3LYP (embedded cluster)		34.9	22.6	16
DFT-LDA/GGA-BP88 (embedded cluster)	Point Ch.(+4/−2)	67.3		45
	Point Ch.(+2/−1)	55.5		
	Fract. Point Ch.	20.8		
DFT-GGA-PW91, 750 eV, 5 Ti layer slab		20.1[a]	21.0[a]	15
		22.8[b]	21.0[b]	
DFT-GGA-RPBE, 400 eV, 7 Ti layer slab		9.2[a]	9.7[a]	49
			8.5[b]	
experiment		14−24		50

[a] At half-monolayer coverage. [b] At monolayer coverage. [c] Extrapolated to zero coverage limit.

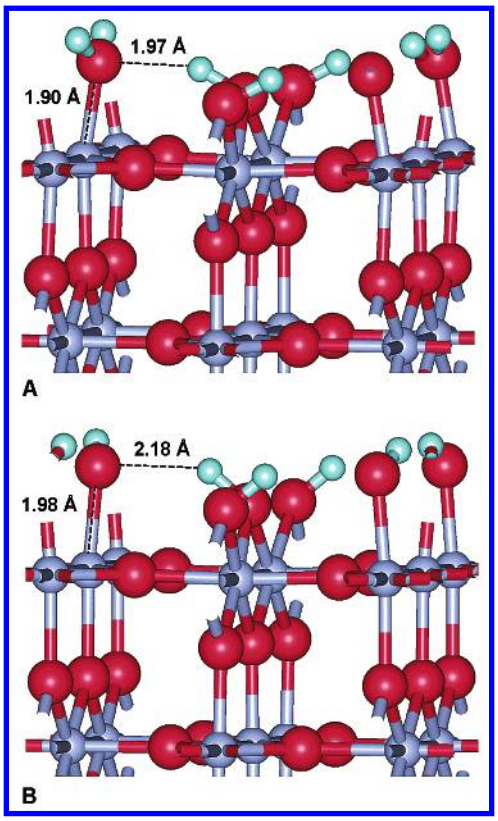

Figure 10. Optimized structure of hydroxylated 3-layer slab with fixed positions of the central plane atoms (model II, full-monolayer coverage) using (A) CASTEP-DFT-GGA-PW91-340 eV and (B) force field calculations.

and 5-layer TiO_2 slabs using our derived force fields for Ti−O interactions. The use of an equal number of H_2O molecules on each side creates a system with minimal dipole moment associated with the slab. The force field results were compared with the results of GGA-PW91 computations for 3-layer slabs in Figures 11 and 12 (Note that a 340 eV cutoff was used in this CASTEP calculation). The distance between Ti^V and the oxygen in H_2O (2.20 Å for half-monolayer coverage and 2.31 for monolayer coverage) calculated with the force field compares well to our DFT calculation (2.17 and 2.26 Å, respectively) and to ab initio results (2.25 Å) using an embedded cluster approach.[16] Also, the DFT orientation of water molecules is well reproduced in both cases.

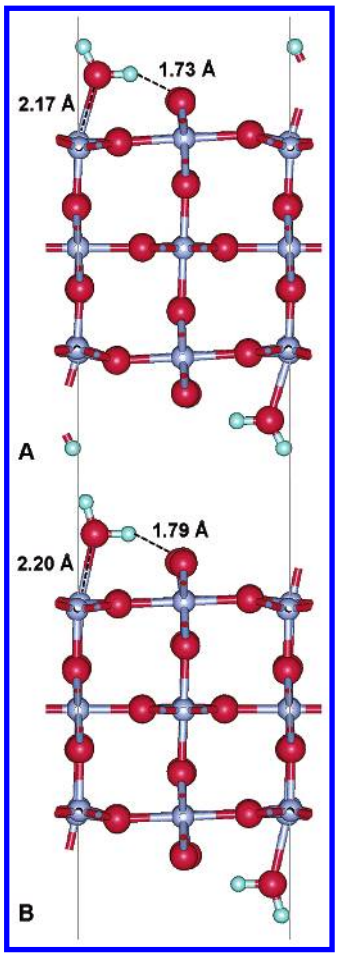

Figure 11. Optimized structure of 3-layer slab with two water molecules (model II) using (A) CASTEP-DFT-GGA-PW91-340 eV and (B) force field calculations.

The adsorption energy of an H_2O molecule (in associated and dissociated forms) to the 3-layer TiO_2 slab was also calculated with the force field and DFT (without a zero-point energy correction). To obtain the DFT value, a GGA-PW91 geometry optimization was carried out for an isolated H_2O molecule. In Table 11, the results on water adsorption energies derived by different methods are compared. Table 11 gives most theoretical values known to us, including those recently obtained by Zhang et al.[49] in their comprehensive study of multilayer

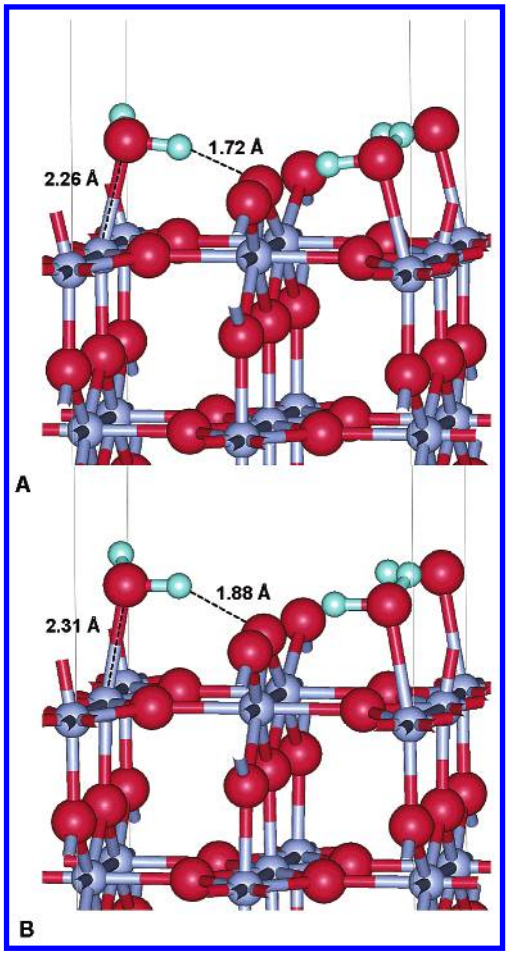

Figure 12. Optimized structure of 3-layer slab with four water molecules (model II) using (A) CASTEP-DFT-GGA-PW91-340 eV and (B) force field calculations.

adsorption. This work shows that H-bond lengths between an adsorbed water molecule and the neighboring bridging oxygens are approximately 1.8 Å, in accord with our calculations as well as the H_2O molecular orientations and H-bond directions (Figures 11 and 12). The data in Table 11 show strong dependence of the calculated adsorption energies on the DFT functional used. Our DFT calculated values for associative and dissociative adsorption energies (21.5−24.9 and 18.4−26.5 kcal/mol, respectively) fall within the experimentally observed range (14−24 kcal/mol;[50]). The associative adsorption energy using the derived force field is slightly larger (25.2−28.9 kcal/mol) than DFT calculations and experiment. Figure 11 shows that DFT calculations predict for model II an H-bond distance of 1.73 Å, whereas the force field predicts 1.79 Å. The Ti−OH_2 bond length is similar in both cases (2.17 vs 2.20 Å), so it probably is not a major source of error in the calculated adsorption energy.

Conclusions

Using DFT theory, we have calculated various models of a relaxed in vacuo rutile (110) surface. Several cases for adsorption of water molecules have been considered. The force field of Matsui and Akaogi for bulk TiO_2 polymorphs has been extended to describe the surface relaxation and water adsorption. In general, the derived force field correctly predicts geometry and energy of the regarded interactions and can be used in molecular dynamic simulations of water-rutile interface.

Acknowledgment. This research was supported by the U.S. Department of Energy, Office of Basic Energy Sciences, Division of Chemical Sciences, Geosciences and Biosciences, under the project "Nanoscale Complexity at the Oxide-Water Interface" and by NSF grant EAR-0073722 "Adsorption of cations on mineral-aqueous solution interfaces at elevated temperatures".

References and Notes

(1) Dohrmann, J. K.; Schaaf, N. S. Energy-conversion by photoelectrolysis of water−Determination of efficiency by in situ photocalorimetry. *J. Phys. Chem.* **1992**, *96*, 4558−4563.

(2) Serpone, N.; Lawless, D.; Disdier, J.; Herrmann, J. M. Spectroscopic, photoconductivity, and photocatalytic studies of TiO_2 colloids−Naked and with the lattice doped with Cr^{3+}, Fe^{3+}, and V^{5+} cations. *Langmuir* **1994**, *10*, 643−652.

(3) Franke, R.; Franke, C. Model reactor for photocatalytic degradation of persistent chemicals in ponds and wastewater. *Chemosphere* **1999**, *39*, 2651−2659.

(4) Li, X. Z.; Li, F. B. Study of Au/Au^{3+}-TiO_2 photocatalysts toward visible photooxidation for water and wastewater treatment. *Environ. Sci. Technol.* **2001**, *35*, 2381−2387.

(5) Ruus, R.; Kikas, A.; Saar, A.; Ausmees, A.; Nommiste, E.; Aarik, J.; Aidla, A.; Uustare, T.; Martinson, I. Ti 2p and O 1s X-ray absorption of TiO_2 polymorphs. *Solid State Commun.* **1997**, *104*, 199−203.

(6) Oliver, P. M.; Watson, G. W.; Kelsey, E. T.; Parker, S. C. Atomistic simulation of the surface structure of the TiO_2 polymorphs rutile and anatase. *J. Mater. Chem.* 1997, *7* (3), 563−568.

(7) Swamy, V.; Gale, J. D.; Dubrovinsky, L. S. Atomistic simulation of the crystal structures and bulk moduli of TiO_2 polymorphs. *J. Phys. Chem. Solids* **2001**, *62*, 887−895.

(8) Henderson, M. A. An HREELS and TPD study of water on TiO_2-(110): the extent of molecular versus dissociative adsorption. *Surf. Sci.* **1996**, *355*, 151−166.

(9) Henderson, M. A. Structural sensitivity in the dissociation of water on TiO_2 single-crystal surfaces. *Langmuir* **1996**, *12* (21), 5093−5098.

(10) Reinhardt, P.; Hess, B. A. Electronic and geometrical structure of rutile surfaces. *Phys. Rev. B* **1994**, *50* (16), 12015−12024.

(11) Ramamoorthy, M.; Vanderbilt, D.; King-Smith, R. D. First-principles calculations of the energetics of stoichiometric TiO_2 surfaces. *Phys. Rev. B* **1994**, *49*, 16721−16727.

(12) Lindan, P. G. D.; Harrison, N. M.; Gillan, M. J.; White, J. A. First-principles spin-polarized calculations on the reduced and reconstructed TiO_2-(110) surface. *Phys. Rev. B* **1997**, *55* (23), 15919−15927.

(13) Bates, S. P.; Kresse, G.; Gillan, M. J. A systematic study of the surface energetics and structure of TiO_2(110) by first-principles calculations. *Surf. Sci.* **1997**, *385* (2−3), 386−394.

(14) Lindan, P. J. D.; Harrison, N. M.; Holender, J. M.; Gillan, M. J. First-principles molecular dynamics simulation of water dissociation on TiO_2(110). *Chem. Phys. Lett.* **1996**, *261* (3), 246−252.

(15) Lindan, P. J. D.; Harrison, N. M.; Gillan, M. J. Mixed dissociative and molecular adsorption of water on the rutile (110) surface. *Phys. Rev. Lett.* **1998**, *80* (4), 762−765.

(16) Stefanovich, E. V.; Truong, T. N. Ab initio study of water adsorption on TiO_2(110): molecular adsorption versus dissociative chemisorption. *Chem. Phys. Lett.* **1999**, *299* (6), 623−629.

(17) Matsui, M.; Akaogi, M. Molecular dynamics simulation of the structural and physical properties of the four polymorphs of TiO_2. *Mol. Simul.* **1991**, *6*, 239.

(18) Kim, D. W.; Enomoto, N.; Nakagawa, Z.; Kawamura, K. Molecular dynamic simulation in titanium dioxide polymorphs: Rutile, brookite, and anatase. *J. Am. Ceram. Soc.* **1996**, *79* (4), 1095−1099.

(19) Yin, X. L.; Miura, R.; Endou, A.; Gunji, I.; Yamauchi, R.; Kubo, M.; Stirling, A.; Fahmi, A.; Miyamoto, A. Structure of TiO_2 surfaces: a molecular dynamics study. *Appl. Surf. Sci.* **1997**, *119* (3−4), 199−202.

(20) Berendsen, H. J. C.; Grigera, J. R.; Straatsma, T. P. The missing term in effective pair potentials. *J. Phys. Chem.* **1987**, *91* (24), 6269−6271.

(21) Perdew, J. P. Unified Theory of Exchange and Correlation Beyond the Local Density Approximation. In *Electronic structure of solids '91*; Ziesche, P., Eschrig, H., Eds.; Akademic Verlag: Berlin, 1991; pp 11−20.

(22) *CASTEP*, Cambridge Serial Total Energy Package, Version 4.2, 1999, Cerius^2 Users Guide, Accelrys (formerly Molecular Simulations Inc.), San Diego, CA.

(23) Vanderbilt, D. Soft self-consistent pseudopotentials in a generalized eigenvalues formalism. *Phys. Rev. B* **1990**, *41*, 7892−7895.

(24) Monkhorst, H. J.; Pack, J. D. Special points for Brillouin-zone integrations. *Phys. Rev. B* **1976**, *13* (12), 5188−5192.

(25) Delley, B. An all-electron numerical method for solving the local density functional for polyatomic molecules. *J. Chem. Phys.* **1990**, *92*, 508−517.

(26) Breneman, C. M.; Wiberg, K. B. Determination atom-centered monopoles from molecular electrostatic potentials. The need for high sampling density in formamide conformational analysis. *J. Comput. Chem.* **1990**, *11*, 361−373.

(27) Dick, B. G.; Overhauser, A. W. Theory of the dielectric constants of alkali halide crystals. *Phys. Rev.* **1958**, *112* (1), 90−103.

(28) Baram, P. S.; Parker, S. C. Atomistic simulation of hydroxide ions in inorganic solids. *Philos. Mag. B* **1996**, *73* (1), 49−58.

(29) Fleming, S.; Rohl, A.; Lee, M.-Y.; Gale, J.; Parkinson, G. Atomistic modeling of gibbsite surface structure and morphology. *J. Cryst. Growth* **2000**, *209*, 159−166.

(30) de Leeuw, N. H.; Parker, S. C. Computer simulation of dissociative adsorption of water on CaO and MgO surfaces and the relation to dissolution. *Res. Chem. Int.* **1999**, *25* (2), 195−211.

(31) de Leeuw, N. H.; Parker, S. C. Effect of chemisorption and physisorption of water on the surface structure and stability of alpha-alumina. *J. Am. Ceram. Soc.* **1999**, *82* (11), 3209−3216.

(32) Liew, C. C.; Inomata, H.; Arai, K. Flexible molecular models for molecular dynamics study of near and supercritical water. *Fluid Phase Equilib.* **1998**, *144* (1−2), 287−298.

(33) Toukan, K.; Rahman, A. Molecular-dynamics study of atomic motions in water. *Phys. Rev. B* **1985**, *31*, 2643−2648.

(34) Frisch, M. J.; et al. *Gaussian 98*, revision A.7; Gaussian, Inc.: Pittsburgh, PA, 1998.

(35) Becke, A. D. Density-functional exchange-energy approximation with correct asymptotic behavior. *Phys. Rev. A* **1988**, *38*, 3098−3100.

(36) Lee, C.; Yang, W.; Parr, R.; Development of the Colle-Salvetti correlation-energy formula into a functional of the electron density. *Phys. Rev. B* **1988**, *37*, 785−789.

(37) Gale, J. D. GULP—a computer program for the symmetry adapted simulations of solids. *J. Chem. Soc., Faraday Trans.* **1997**, *93*, 629.

(38) Curtiss, L. A.; Halley, J. W.; Hautman, J.; Rahman, A. Nonadditivity of ab initio pair potential for molecular dynamics of multivalent transition metal ions in water. *J. Chem. Phys.* **1987**, *86*, 2319−2327.

(39) Guardia, E.; Padro, J. A. Molecular dynamics simulation of ferrous and ferric ions in water. *Chem. Phys.* **1990**, *144*, 353−362.

(40) Fowler, P. W.; Harding, J. H.; Pyper, N. C. The polarizabilities and dispersion coefficients for ions in the solid group IV oxides. *J. Phys.: Condens. Matter* **1994**, *6*, 10593−10606.

(41) Calderwood, J. H. A classical electrostatic model for tetragonal single crystals of barium titanate. *Philos. Trans. R. Soc. London* **1997**, *A 355*, 1−42.

(42) Cohen, R. C.; Saykally, R. J. Determination of an improved intermolecular global potential-energy surface for $Ar-H_2O$ from vibration−rotation-tunneling spectroscopy. *J. Chem. Phys.* **1993**, *98*, 6007−6030.

(43) Bergstrom, R.; Lunell, S. Comparative study of DFT methods applied to small titanium/oxygen compounds. *Int. J. Quantum Chem.* **1996**, *59* (6), 427−443.

(44) Vogtenhuber, D.; Podloucky, R.; Redinger, J. Ab initio studies of H_2O adsorption on the TiO_2(110) rutile surface. *Surf. Sci.* **1998**, *404* (1−3), 798−801.

(45) Casarin, M.; Maccato, C.; Vittadini, A. Molecular chemisorption on TiO_2(110): A local point of view. *J. Phys. Chem. B* **1998**, *102* (52), 10745−10752.

(46) Goniakowski, J.; Gillan, M. J. The adsorption of H_2O on TiO_2 and SnO_2(110) studied by first-principles calculations. *Surf. Sci.* **1996**, *350* (1−3), 145−158.

(47) Evarestov, R. A.; Bandura, A. V. Unpublished results.

(48) Stefanovich, E. V.; Shluger, A. L. (100) GaP surface charges, potentials, and stoichiometry; a quantum-chemical study. *J. Phys.: Condens. Matter* **1994**, *6*, 4255−4268.

(49) Zhang, C.; Lindan, P. J. D. Multilayer water adsorption on rutile TiO_2(110): A first-principles study. *J. Chem. Phys.* **2003**, *118*, 4620−4629.

(50) Brinkley, T.; Dietrich, M.; Engel, T.; Farrall, P.; Gantner, G.; Schafer, A.; Szuchmacher, A. A modulated molecular beam study of the extent of dissociation of H_2O on TiO_2(110). *Surf. Sci*. **1998**, *395*, 292−306.